

Proteomic landscape of primary and metastatic brain tumors for heterogeneity discovery

Shuang Yang¹, Chengbin Zhou², Lei Zhang³, Yueting Xiong³, Yongtao Zheng², Liuguan Bian², and xiaohui liu¹

¹Affiliation not available

²Shanghai Jiao Tong University

³Fudan University

January 30, 2024

Abstract

Purpose: Brain tumors, whether primary or secondary, have limited information about proteomic changes despite advances in the understanding of the driver gene mutations and heterogeneity within tumor cells. The purpose of this study is to distinguish primary and secondary brain tumors based on proteomics. **Experimental Design:** We assembled the most common primary tumors as follows: gliomas from WHO grade II to IV with or without IDH1 mutations; and BrMs with a wide range, including lung cancer (L.C), breast cancer (B.C), ovarian cancer (O.C), and colorectal cancer (C.C). A total of 29 tissue samples were analyzed by label free quantitative mass spectrometry-based proteomics. **Results:** In total, 8,370 protein groups were identified, and approximately 4,000 quantified protein groups were adopted for further analysis. Proteomic analysis of metastatic tumors reveals conserved features across multiple cancers. While proteomic heterogeneities were found for discriminating low- and high-grade of gliomas, as well as IDH1 mutant and wild-type gliomas. And distinct pathway-level differences among these two types of brain malignancies were revealed. The characteristic pathways of BrMs focused on proliferation and immunomodulation after colonizing the brain, whereas invasion processes were notably activated in gliomas. **Conclusions and Clinical Relevance:** We elucidated an extensive proteomic landscape of BrMs and gliomas, providing information for the development of potential therapeutic and diagnostic strategies for type-specific brain tumors.

Proteomic landscape of primary and metastatic brain tumors for heterogeneity discovery

Shuang Yang^{1*}, Chengbin Zhou^{2*}, Lei Zhang¹, Yueting Xiong¹, Yongtao Zheng², Liuguan Bian², Xiaohui Liu¹

¹The Fifth People's Hospital of Shanghai, Shanghai Key Laboratory of Medical Epigenetics, The International Co-laboratory of Medical Epigenetics and Metabolism, Ministry of Science and Technology, Institutes of Biomedical Sciences, Fudan University, Shanghai, 200032, China

² Department of Neurosurgery, Ruijin Hospital, School of Medicine, Shanghai Jiao Tong University, Shanghai, 200025, China.

* Contributed equally to this work.

Corresponding Author

Xiaohui Liu, The Fifth People's Hospital of Shanghai, Shanghai Key Laboratory of Medical Epigenetics, The International Co-laboratory of Medical Epigenetics and Metabolism, Ministry of Science and Technology, Institutes of Biomedical Sciences, Fudan University, Shanghai, 200032, China; Tel: +86-021-65642009; E-mail: liuxiaohui@fudan.edu.cn

Abstract

Purpose: Brain tumors, whether primary or secondary, have limited information about proteomic changes despite advances in the understanding of the driver gene mutations and heterogeneity within tumor cells. The purpose of this study is to distinguish primary and secondary brain tumors based on proteomics.

Experimental Design: We assembled the most common primary tumors as follows: gliomas from WHO grade II to IV with or without *IDH1* mutations; and BrMs with a wide range, including lung cancer (L.C), breast cancer (B.C), ovarian cancer (O.C), and colorectal cancer (C.C). A total of 29 tissue samples were analyzed by label free quantitative mass spectrometry-based proteomics.

Results: In total, 8,370 protein groups were identified, and approximately 4,000 quantified protein groups were adopted for further analysis. Proteomic analysis of metastatic tumors reveals conserved features across multiple cancers. While proteomic heterogeneities were found for discriminating low- and high-grade of gliomas, as well as *IDH1* mutant and wild-type gliomas. And distinct pathway-level differences among these two types of brain malignancies were revealed. The characteristic pathways of BrMs focused on proliferation and immunomodulation after colonizing the brain, whereas invasion processes were notably activated in gliomas.

Conclusions and Clinical Relevance: We elucidated an extensive proteomic landscape of BrMs and gliomas, providing information for the development of potential therapeutic and diagnostic strategies for type-specific brain tumors.

KEYWORDS

brain metastasis, glioma, biomarker, proteomics, liquid chromatography tandem mass spectrometry

1 INTRODUCTION

The brain, as the major organ of the central nervous system (CNS), controls and processes most of the body's activities. Therefore, the most malignant brain tumors, namely, glioblastomas (GBMs) and brain metastases (BrMs), from extracranial primary tumors (such as lung, breast, melanoma, and colorectal cancers) are among the deadliest cancers with poor prognosis and short survival [1]. At present, an effective treatment option for patients with malignant brain tumors has long presented a challenge for oncologists.

Gliomas are one of the most prevalent tumors in the CNS with disproportionate mortality and morbidity among subtypes. The most commonly occurring types of gliomas are astrocytoma (WHO grade I - IV), oligodendroglioma (WHO grade II - III), and GBM [2, 3]. Glioma alterations, such as isocitrate dehydrogenase (*IDH*) 1 and 2 mutations as well as *1p/19q* codeletion, generally occur in low grade gliomas (II or III) and provide superior prognostication compared to *IDH* wild-type tumors [4, 5]. Despite routine therapies, such as surgical resection, radiation, and chemotherapy, the outcomes of patients remain poor. The median survival rates of glioma patients are stubbornly low, varying from years (WHO grade II) to months (WHO grade IV) [6].

BrMs are 10 times more common than primary brain tumors with 10-30% incidence in adults, and they have an even lower survival rate that is typically measured in months [7, 8]. Fewer than 10% of all BrMs are found before the primary cancer is diagnosed. The determination of whether extracranial tumors develop BrMs relies mainly on cranial imaging [magnetic resonance imaging (MRI) or computed tomography (CT)], which has a severe time lag from diagnosis to treatment, causing the optimal therapeutic timeframe to be missed [9, 10]. In addition, although these two representative primary and secondary brain tumors exhibit markedly different modes of antigen presentation and tumor microenvironment [11], there is no effective molecular marker to assist in distinguishing these two types of brain tumors. The pathological diagnosis is confirmed

by immunohistochemistry from tumor tissue obtained after surgery or a biopsy, which delays intervention and precise treatment selection. Consequently, accurate preoperative discrimination of BrM and glioma is critical for individualized therapeutic decision-making.

Markers found in the blood and tissue samples have been utilized for the diagnosis of the primary disease and to guide treatment. Recent studies applying immunohistochemistry, genome-wide transcriptomics, and single-cell transcriptomics to investigate BrMs and gliomas have had a profound impact on cancer biology [12-16]. Klemm et al. constructed a high-dimensional, multi-omics characterization of the brain tumor microenvironment, allowing elucidation of the disease- and cell type-specific expression patterns of gliomas and BrMs [17]. However, there are still challenges that hinder the transition of these findings into new effective therapies. Potential explanations for the disconnect between genomics-based studies and clinical trials include the lack of protein information and the poor correlation between protein and mRNA expression (0.54) [18, 19]. As the main carrier and executor of life activities, protein shows a more direct connection with the occurrence and development of diseases. Despite some transcriptomic studies, the precise proteomic composition of these two distinct human brain malignancies, especially BrMs, remains unclear. Thus, an integrated and in-depth proteomic analysis is required for the comprehensive understanding of these brain cancers.

Mass spectrometry (MS)-based proteomics is an integral part of cancer research, shedding light on the functional profile of the cancer cell. The present study demonstrated for the first time a systematic proteomic analysis of two typical malignant brain tumors, namely BrMs and gliomas. We generated and analyzed a comprehensive catalog of the disease type-specific protein expression patterns as a resource for the research community, and we also investigated their interrelationships.

2 MATERIAL AND METHODS

2.1 Chemicals and reagents

Acetonitrile (ACN, MS grade), trifluoroacetic acid (TFA, MS grade), formic acid (FA, MS grade), Pierce™ BCA Protein Assay Kit and HeLa Protein Digest Standard were purchased from Thermo Scientific (St. Louis, MO, USA). Culture media such as Dulbecco's Modified Eagle's Medium (DMEM), penicillin/streptomycin (P/S), fetal bovine serum (FBS) and trypsin-EDTA were from Gibco Life Technologies (New York, USA). The iST kit for proteomic sample preparation was purchased from PreOmics GmbH (Planegg, Germany). Deionized water used in the experiments was prepared by the Milli-Q50SP system (Millipore, Milford, MA).

2.2. Patients and sample collection

The present study was conducted in accordance with the guidelines of the Declaration of Helsinki with the approval of the Research Ethics Committee from Ruijin Hospital, Shanghai Jiaotong University School of Medicine (1.0/2019-10-1). Written informed consent was obtained from all patients or their legal representatives prior to their participation in the study.

A total of 29 samples from gliomas and BrMs patients were obtained from the Ruijin Hospital, Shanghai Jiao Tong University School of Medicine between October 2020 and September 2021. Details of clinical information on the subjects were shown in Figure 2A and Table S1. Tumor tissues were collected after surgery, and were washed three times with PBS. After that, tissues were immediately transferred to liquid nitrogen and collected into 2 mL cryogenic storage vials (Corning, New York, USA), and stored at -80 °C for later use.

2.3. Cell culture and collection

The human cervical cancer cell line, HeLa (ATCC, USA), was cultured at 37 °C and 5% CO₂ in DMEM with 10% FBS and 1% penicillin/streptomycin. The culture medium was refreshed every 2 - 3 days. Cells were harvested at >80% confluency following treatment with 0.25% trypsin-EDTA solution to obtain a cell suspension. Cells were dispersed in growth medium, and the cell density was measured by an automated cell counter (Cellometer AutoT4, Nexcelom, USA). The defined number of cells was washed three times with

ice-cold PBS and centrifuged at 1000 rpm for 10 min at 4 °C. Cells were then placed into 1.5-mL protein LoBind tubes (5 X 10⁵ cells per tube) and stored at -80 degC for future analysis.

2.4. Sample preparation based on iST kit

Glioma and BrM tissues from patients as well as HeLa cells were prepared according to the iST kit manufacturer's instructions [20]. Briefly, tissue samples were cut and weighed, and 1 mg of each tissue sample was placed into a clean 1.5-mL protein LoBind tube followed by the addition of 100 µL of LYSE and incubation at 95 °C for 30 min with shaking (1000 rpm). HeLa cells for the experimental control were treated simultaneously. The sample was sheared using a sonicator (10 cycles; 30 sec ON/OFF), and protein concentration was determined using the PierceTM BCA Protein Assay Kit. An equal amount of protein (100 µg) for each sample was used for digestion. Then, 210 µL of RESUSPEND was added to DIGEST followed by shaking at room temperature for 10 min at 500 rpm. Then, 50 µL of DIGEST was added to the sample and heated using a pre-heated heating block at 37 °C for 3 h at 500 rpm. After digestion, 100 µL of STOP was added to the sample followed by shaking at room temperature for 10 min at 500 rpm. The sample was then centrifuged at 14,000 rpm for 1 min, and the sample was then serially washed with 200 µL of WASH 0, WASH 1, and WASH 2 for desalting. Then, 100 µL of ELUTE was added twice to elute peptides, and the peptides were lyophilized to dryness and stored at -20 °C or redissolved in 0.1% FA for nano-LC-MS/MS analysis.

2.5. Nano-LC-MS/MS analysis

Liquid chromatography tandem mass spectrometry (LC-MS/MS) analysis was performed on a timsTOF mass spectrometer with PASEF (Bruker Daltonics, Bremen, Germany) coupled to a Nano Elute liquid chromatograph (Bruker Daltonics, Bremen, Germany) with a 75 µm × 25 cm-long column (1.6 µm id, Dr. Maisch GmbH, Germany). Peptide separation was performed at a flow rate of 200 nL/min with mobile phases A (0.1% FA in water) and B (0.1% FA in ACN) in the following 90 min gradient: 0 - 70 min, 2% - 22% B; 70 - 80 min, 22 - 37% B; 80 - 82 min, 37% - 80% B; and 82 - 90 min, 80% B.

Peptides were acquired in the data-dependent acquisition mode (DDA). The following parameters were used: mass range, 100 to 1700 m/z; 1/K0 start at 0.7 V[?]/s/cm² and end at 1.3 V[?]/s/cm²; capillary voltage, 1500 V; dry gas, 3 L/min; and dry temp, 180 °C. The PASEF settings were as follows: 4 MS/MS scans (total cycle time 0.53 sec); charge range, 0 - 5; active exclusion, 0.4 min; scheduling target intensity, 20000; intensity threshold, 2500; and CID collision energy started at 27 eV and ended at 45 eV.

2.6. Database search

All raw data were analyzed by Peaks online (X build 1.7.2022-03-24_170623). The following parameters were used: MS 1 tolerance, 10 ppm; MS2 tolerance, 0.02 Da; and searched database, UniProt-human database (20,375 entries) for the tumor tissue as well as HeLa samples. A false discovery rate (FDR) lower than 1% was used as the cutoff value for the peptide, protein, and propensity score matching (PSM) identification based on the target decoy strategy. Carbamidomethylation of cysteine was considered a fixed modification, and protein N-terminal acetylation, oxidation of methionine, and deamidation of asparagine and glutamine were considered as variable modifications.

2.7. Data analysis

LFQ data were normalized by total ion current (TIC) and filtered for 50% valid intensity values across all samples. Missing values were replaced by 1/5 of the minimum positive value of each variable by MetaboAnalyst 5.0 [21]. Quantified proteins with fold change > 2 or < 0.5 and P value < 0.05 were considered as DEPs. In the figures, experimental data are shown as standard error of mean.

Metascape [22] was utilized for functional enrichment and protein-protein interaction networks analysis. P values for the functional enrichments were calculated by a hypergeometric test and corrected by the Benjamini-Hochberg FDR method. Cytoscape [23] software was used for reorganizing and visualizing the interaction networks. The proportional Venn diagrams and the Sankey diagram were analyzed using a Bioinformatics online tool. The artwork was created with BioRender.com. MetaboAnalyst 5.0 [21] was used for

the statistical analysis and biomarker discovery of DEPs, including unsupervised clustering, PCA, Pearson correlation analysis, and machine learning.

For machine learning, ROC curves were generated using MetaboAnalyst 5.0. Multivariate ROC curves were generated by Monte Carlo cross-validation (MCCV) using balanced sub-sampling. In each MCCV, two-thirds of the samples were used to evaluate the feature importance. The top 2, 3, 5, 10 ... 100 (max) important features were then used to build classification models, which were validated using one-third of the remaining samples. The procedure was repeated multiple times to calculate the performance and confidence interval of each model. PLS-DA was used as the classification method, and the PLS-DA built-in was selected as the feature-ranking method with two latent variables. Feature selection was based on the ROC curve results, and the top 5, 10, 15, 25, 50, and 100 proteins were used for predictive accuracy assessment.

3 RESULTS

3.1 Overall proteomic analysis of brain tumors

In an attempt to analyze the proteome of primary and secondary tumors, we assembled the most common primary tumors as follows (Figure 1): gliomas from WHO grade II to IV with or without *IDH1* mutations; and BrMs with a wide range, including lung cancer (L.C), breast cancer (B.C), ovarian cancer (O.C), and colorectal cancer (C.C). Figure 2A and B, as well as Table S1 provide additional details for the assembled cohort and MRI for diagnosis.

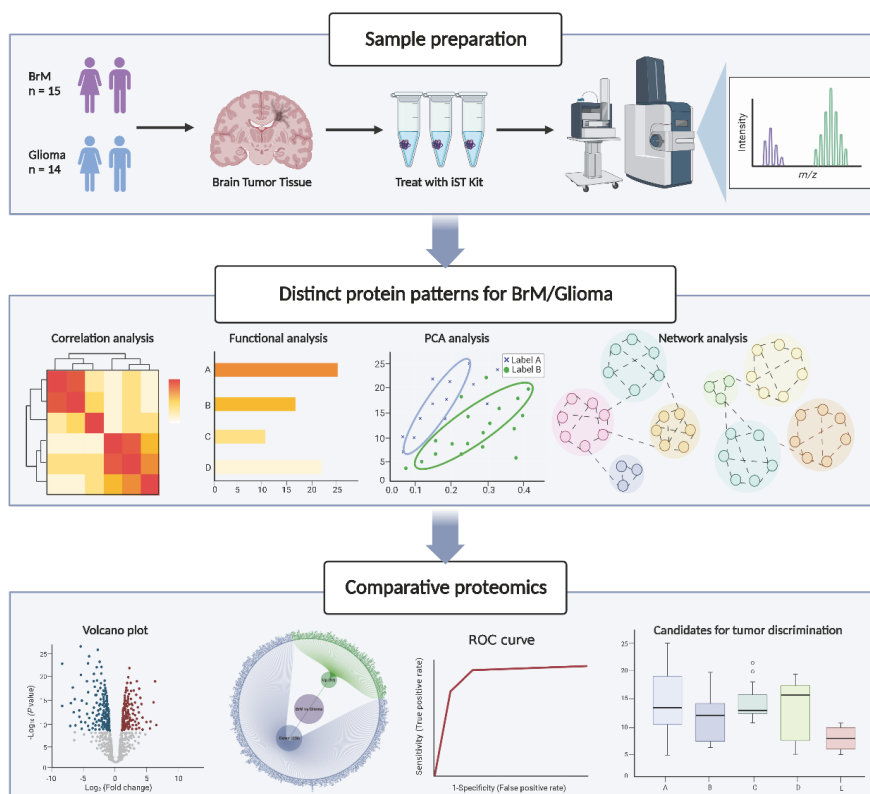


FIGURE 1 Schematic diagram of the workflow. Proteomic samples were prepared and analyzed by mass spectrometry. The protein profiles of the two types of brain tumors were discussed separately, followed by comparative analysis to find potential biomarkers that could distinguish between the two tumors of different origin.

During the MS acquisition, four commercial HeLa digests (200 ng each) were uniformly inserted for monitoring MS for instrumental quality control (QC), which showed a constant stability across the entire process of sample analysis (Figure 2C, Figure S1A and B). In addition, three HeLa samples (H) were treated in parallel with tumor tissues from sample preparation to data analysis. Two types of tumors were analyzed alternately at random, and the HeLa sample was inserted every 10 samples for quality control, resulting in an average of approximately 5200 identified proteins and 4499 co-quantified proteins in HeLa cells (Figure S1C and D). Furthermore, a similar distribution of peptide intensities, low coefficient of variation (CV), and high correlation (0.99) of LFQ proteins were observed in the three HeLa samples (Figure 2D, Figure S1E-G). Overall, we performed robust proteomic analysis for two types of brain tumors using rigorous experiment controls. As a result, 27 of the 29 cohort samples successfully passed the quality control filters with more than 50% overlap of identified proteins in each sample. In total, 8,370 protein groups and 116,526 peptides were identified across all samples, and averages of 4,200 proteins and 33,000 peptides were recovered per sample (Figure 2E). In addition, the missed cleavage rate was as low as 10% on average (Figure S1H), indicating a well-controlled sample preparation.

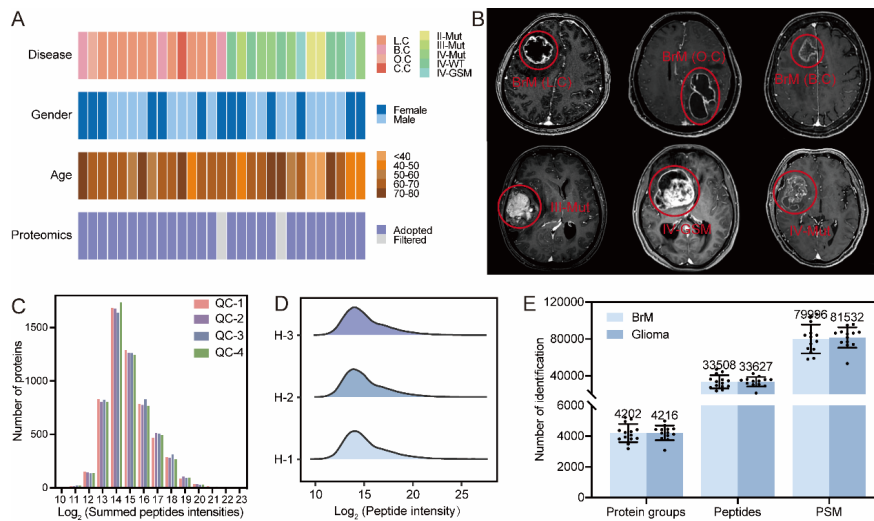
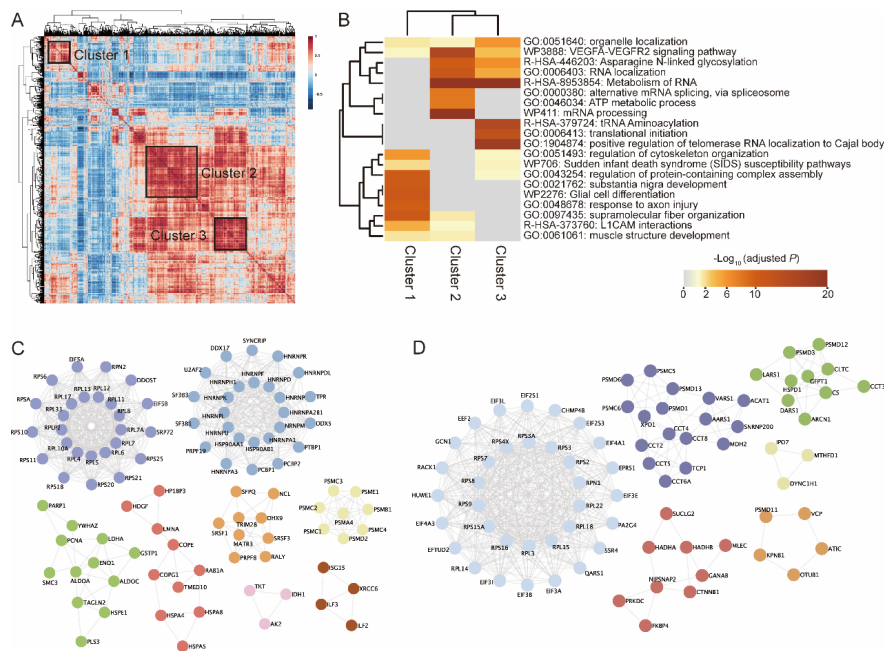


FIGURE 2 System-wide analysis of clinical samples. **A** Heatmap describing samples collected from 29 patients, including gliomas from WHO grade II to IV with or without *IDH1* mutations as well as BrMs from lung cancer (L.C), breast cancer (B.C), ovarian cancer (O.C), and colorectal cancer (CC). In addition, 27 samples were utilized for later analysis with more than 50% overlap of identified proteins in each sample. **B** Contrast-enhanced magnetic resonance imaging (MRI) of BrMs and gliomas. Patients with BrMs from L.C, O.C and B.C as well as gliomas of WHO grade III with *IDH1* mutation (III-Mut), IV with *IDH1* mutation (IV-Mut), and gliosarcoma (IV-GSM) are shown. **C** Number of quantified proteins segregated by binned average protein intensities in four commercial HeLa digests for mass spectrometry quality control (QC). **D** Distribution of peptide intensities in parallel HeLa (H) treatments ($n = 3$) for experimental quality control. **E** Number of protein group, peptide and propensity score matching (PSM) identifications for BrMs ($n = 14$) and gliomas ($n = 13$). Values above columns indicate average numbers of identification. Error bars indicate standard error of mean based on biological replicates.

3.2 Cell proliferation and immune response are conserved features for BrMs

The following four essential hallmarks of metastatic cells during invasion and brain metastasis have been previously proposed: (a) motility and invasion; (b) modulation of the microenvironment; (c) plasticity; and (d) colonization [24]. L.C, B.C, and C.C are the most common types of cancer that metastasize to the brain. Here, we performed unsupervised clustering and searched for robust clustering of distinct features of the proteome correlated with all BrMs to increase our understanding of the general mechanisms of BrMs.

Hierarchical clustering identified 3 clusters across all samples, resulting in 79 proteins in cluster 1, 192 proteins in cluster 2, and 125 proteins in cluster 3 (Figure 3A and Table S2). Functional analysis of the three clusters revealed marked enrichment in cell proliferation for colonization and immune response to modulate the microenvironment (Figure 3B, Figure S2A and B). Importantly, the transcriptomic results of BrMs validate these functions [16].



Specifically, protein groups in cluster 1 were relevant to cell development, such as regulation of cytoskeleton organization, regulation of protein-containing complex assembly, and supramolecular fiber organization. Cluster 2 was characterized by ribosome biogenesis for cell proliferation and immune response to the microenvironment. Ribosomal proteins (RPs) of the 60S (e.g., RPL3, RPL5, and RPL14) and 40S (e.g., RPS6, RPS8, and RPS16) were enriched in clusters 2 and 3 (Figure 3C and D). Cell proliferation-related proteins for pre-mRNA processing (e.g., HNRNPA1, HNRNPK, and HNRNPL), core spliceosome (e.g., SRSF1, SF3B3, and SFPQ), and proteasome complex (e.g., PSMC3, PSMA4, and PSMB1) were present in cluster 2. Moreover, a unit of proteins (ILF2, ILF3, ISG15, and XRCC6) involved in the modulation of the tumor microenvironment by the inflammatory was identified. Further, cluster 3 encompassed energy metabolism and RNA translation for tumorigenesis.

FIGURE 3 Distinct features of BrM proteome profile. **A** Unsupervised clustering of the top 1000 protein features out of 3843 label free quantification (LFQ) proteins based on their interquartile range (IQR) in 14 samples of BrMs. Pearson correlation was used for distance measurement. **B** Gene set enrichment analysis (GSEA) of proteins in the three clusters. The top 20 annotations of GO-BP, Reactome, WikiPathways, and KEGG pathways are shown (Benjamini-Hochberg FDR method, adjusted $P < 0.01$). **C** Protein enrichment networks in cluster 2 based on the top three functional enriched terms (R-HSA-8953854, R-HSA-2262752, and R-HSA-8953897) (Benjamini-Hochberg FDR method, adjusted $P < 0.01$). **D** Protein enrichment networks in cluster 3 based on the top three functional enriched terms (R-HSA-72766, GO:0006412, and GO:0043043) (Benjamini-Hochberg FDR method, adjusted $P < 0.01$).

3.3 Glioma subtypes correlate with respective protein patterns

Although the heterogeneity of gliomas has been described in terms of histochemistry and prognosis [2, 4],

the understanding of low- and high-grade gliomas remains rudimentary to date, and there is no effective diagnostic method based on proteins [25, 26]. In response to the poor diagnostic outcomes in different subtypes of gliomas, we next focused on resolving protein pattern differences among gliomas. Firstly, integrated proteomic analysis of different grades of glioma showed independent and well-separated clusters. Low-grade gliomas (WHO grade II and III) exhibited a close correlation and differed from grade IV gliomas (Figure 4A). Complementarily, gliosarcoma (GSM), a rare form of grade IV gliomas (2%) that has both sarcomatous and malignant glial components [17], was found as a relatively separate entity in principal component analysis (PCA) and even had a closer relationship with grade III glioma when using Pearson correlation (Figure S3A and B). However, in GBMs, no separate clustering between *IDH1* mutation (IV-Mut) and wild type (IV-WT) was observed.

To compare the proteome differences between low- and high-grade gliomas, we grouped WHO grades II and III tumors into a single consolidated low-grade group (II/III-Mut) and compared it to GBMs with *IDH1* mutation (IV-Mut). In total, 36 proteins were aberrantly expressed in IV-Mut versus II/III-Mut ($P < 0.05$), of which 25 proteins were upregulated and 11 proteins were downregulated (Figure 4B and Figure S3B and C). Of note, the downregulated proteins in IV-Mut were associated with poor survival, whereas upregulated proteins were associated with the immune response.

IDH1/2 mutant GBMs are distinct from wild-type GBMs with respect to molecular and clinical features, including prognosis [27, 28]. We next elucidated the proteomic differences between IV-Mut and IV-WT GBMs, which accounted for 66 upregulated proteins and 10 downregulated proteins (Figure S3E). To further investigate these differentially expressed proteins (DEPs), gene set enrichment analysis (GSEA) was performed (Figure 4C). Tumor invasion-related processes (e.g., Rho GTPase cycle, cellular amino acid metabolic process, membrane trafficking, and ferroptosis) were predominately upregulated in IV-Mut. Intriguingly, ferroptosis, a newly discovered form of cell death, is not only correlated with cell migration but also represents a better prognosis in IV-Mut versus IV-WT [29, 30].

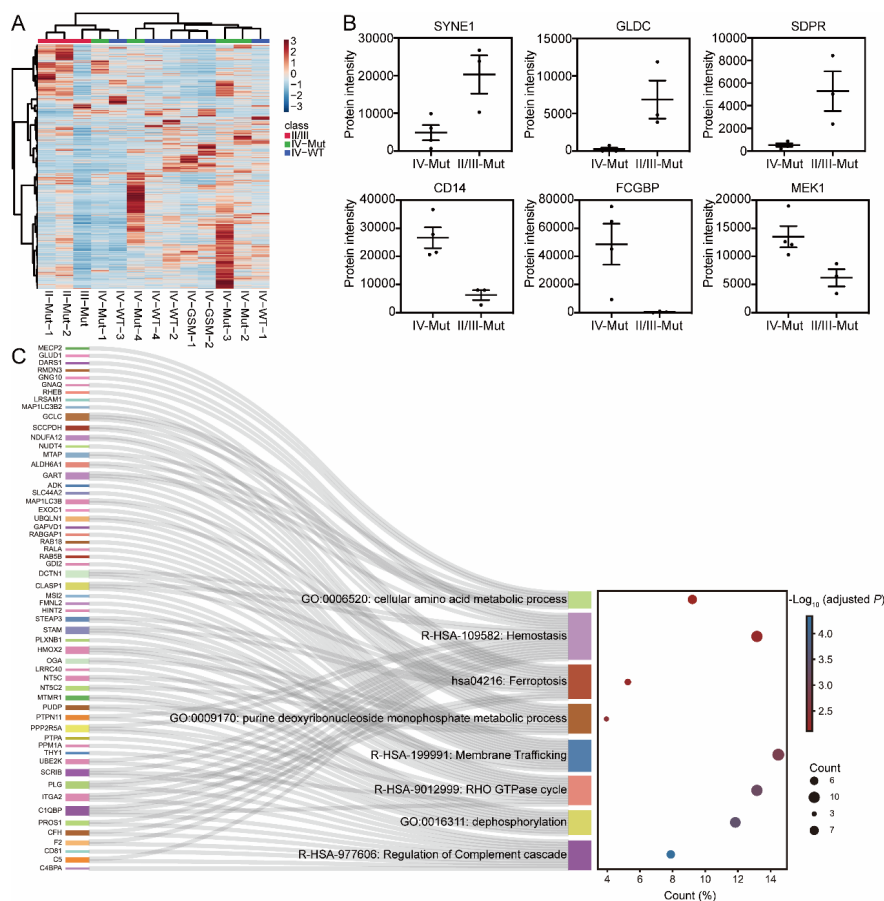


FIGURE 4 Unsupervised clustering of protein patterns distinguishes distinct grades of gliomas. **A** Multigroup heatmap with dendrogram of 4068 LFQ proteins across 13 glioma samples. Ward’s method was performed for clustering, and Pearson correlation was used for distance measurement. **B** Representation of the total intensity of selected proteins (SYNE1, GLDC, SDPR, CD14, FCGBP, and MEK1) of WHO grade IV (IV-Mut, $n = 4$) and II/III (II/III-Mut, $n = 3$) *IDH1* mutant gliomas measured by LC-MS/MS (two-tailed Student’s t-test, $P < 0.05$). Error bars indicate standard error of mean based on biological replicates. **C** Sankey plot showing the GSEA results of differentially expressed proteins (DEPs) in GBMs with *IDH1* mutation (IV-Mut, $n = 4$) and *IDH1* wild type (IV-WT, $n = 4$). The annotations of GO-BP, Reactome, WikiPathways, and KEGG pathways are shown (Benjamini-Hochberg FDR method, adjusted $P < 0.01$).

3.4 Comparative proteomics for primary and secondary brain tumors

Gliomas and BrMs are the most predominant primary and secondary brain tumors in the human brain with a common trait of various malignancies. We next investigated the proteomic heterogeneity of these two types of brain tumors. These two typical brain tumors are composed of unique cell types, anatomical structures, metabolic constraints, and immune environment [17], which may explain the tendency of some extracranial cancers to migrate toward the brain and provide new insights into the blood-brain barrier (BBB) changes during tumor metastasis. For comparative proteomic analysis, malignant brain tumors from primary (gliomas, $n = 13$) and secondary (BrMs, $n = 14$) brain tumors were utilized.

In total, 352 proteins were statistically different between the cohorts ($P < 0.01$), of which 93 proteins were upregulated and 259 proteins were downregulated in BrMs versus gliomas (Figure 5A, Figure S4A and Table

S3). The 352 DEPs effectively distinguished two types of tumors in unsupervised clustering and PCA based on component 1 (96.1%) and component 2 (1.8%) (Figure 5B and Figure S4B).

We next performed functional enrichment analysis for the upregulated and downregulated proteins, respectively (Figure 5C, Figure S4C and D). To some extent, the general cellular and molecular pathways were similar in both types of malignant brain tumors. However, proteins in some distinct pathways were upregulated in BrMs, such as Golgi vesicle transport, formation of the cornified envelope, and secretion (Figure 5C and Figure S4C). Specific processes involved in gliomas were correlated with cell migration, including regulation of actin cytoskeleton, modulation of chemical synaptic transmission, neuron projection development and so on. Taken together, the proteome-based results clearly illustrated that BrM colonization in the brain depends on tumorigenesis and multiple interactions of metastatic cancer cells with the brain microenvironment, whereas gliomas, as one of the representative primary tumors in the brain, maintain a high tendency to invade. These findings prompted further exploration of candidate biomarkers for distinguishing primary and secondary brain tumors.

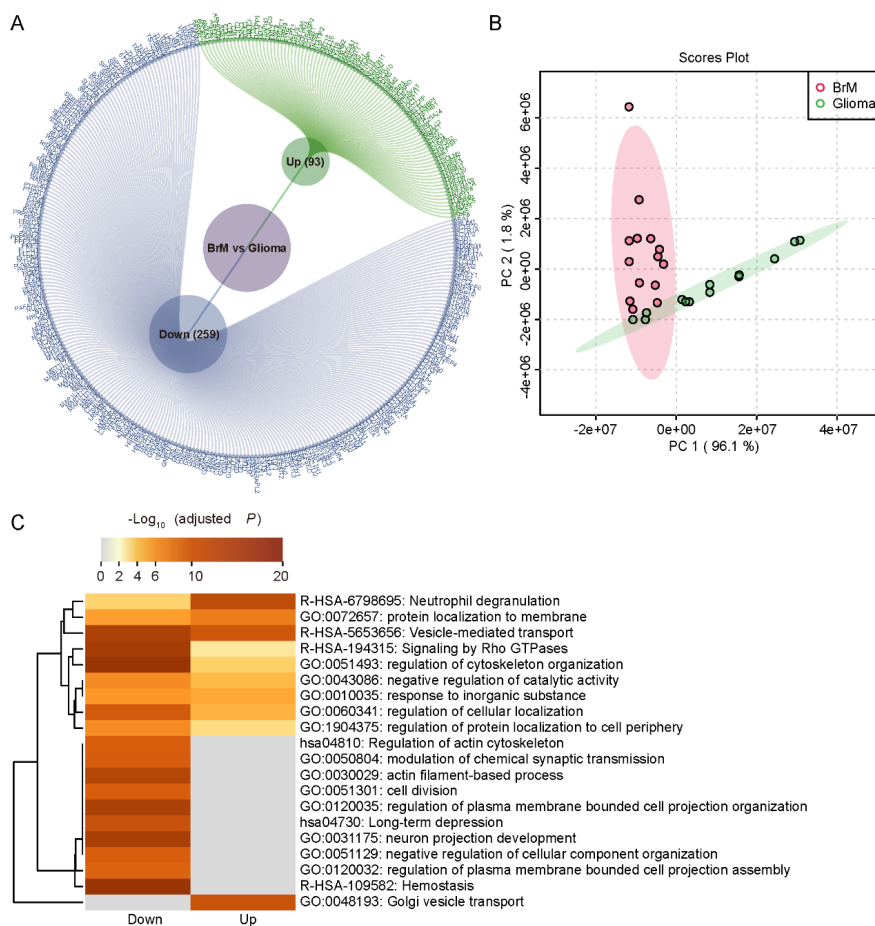


FIGURE 5 Proteomic differences between primary and metastatic brain tumors. **A** Comparison of BrMs ($n = 14$) to gliomas ($n = 13$) identified 352 DEPs (two-tailed Student's t -test, $P < 0.01$ and fold change > 2 or < 0.5). **B** Principal component analysis (PCA) of BrM ($n = 14$) and glioma ($n = 13$) samples based on 352 DEPs. The 95% confidence regions are shown. **C** GSEA identified downregulated and upregulated proteins in the two groups. The top 20 annotations of GO-BP, Reactome, WikiPathways, and KEGG pathways are shown (Benjamini-Hochberg FDR method, adjusted $P < 0.01$).

3.5 Diagnostic classification model for gliomas and BrMs

To illustrate the capacity of proteomic profiling as a powerful prognostic tool for discriminating glioma and BrM tumors, we attempted the diagnostic classification model. To construct a more precise model, malignant brain tumors from primary (WHO grade IV gliomas, glioma (IV), $n = 10$) and secondary (metastases from L.C, BrM (L.C), $n = 10$) tumors were adopted for further analysis, which resulted in 265 DEPs (Figure S5A and B). The DEPs in BrM (L.C) versus glioma (IV) and BrM versus glioma showed high overlap (Figure S5C). In line with the above GSEA results, the most notable pathways of the 265 DEPs were enriched in cell movement (Figure S5D). Of these, 37 proteins accounted for 5.23% of the proteins in the Rho GTPase signaling pathway (R-HSA-194315 and R-HSA-9716542), and 32 proteins comprised up to 8.02% of the proteins in the regulation of the actin filament-based process (GO: 0032970). These results were consistent with the migratory and invasive characteristics of malignant cells.

We next used multivariate receiver operating characteristic (ROC) curve analysis based on partial least squares discriminant analysis (PLS-DA). The above 265 differentially expressed variables were analyzed to obtain the optimal and most economical biomarker combination. Five variables (KRT8, KRT19, KRT7, TACSTD2, and CDH1) reached the most economical and optimal area under the curve (AUC) of 0.973 (95% confidence interval [CI] = 0.803–1) (Figure 6A). To evaluate the reliability of the machine-learning strategy, confusion matrices were generated, and the results demonstrated that different samples were correctly classified with 90% accuracy (Figure 6B and C). Notably, these five proteins were significantly upregulated in the BrM (L.C) samples compared to the glioma (IV) samples (Figure 6D).

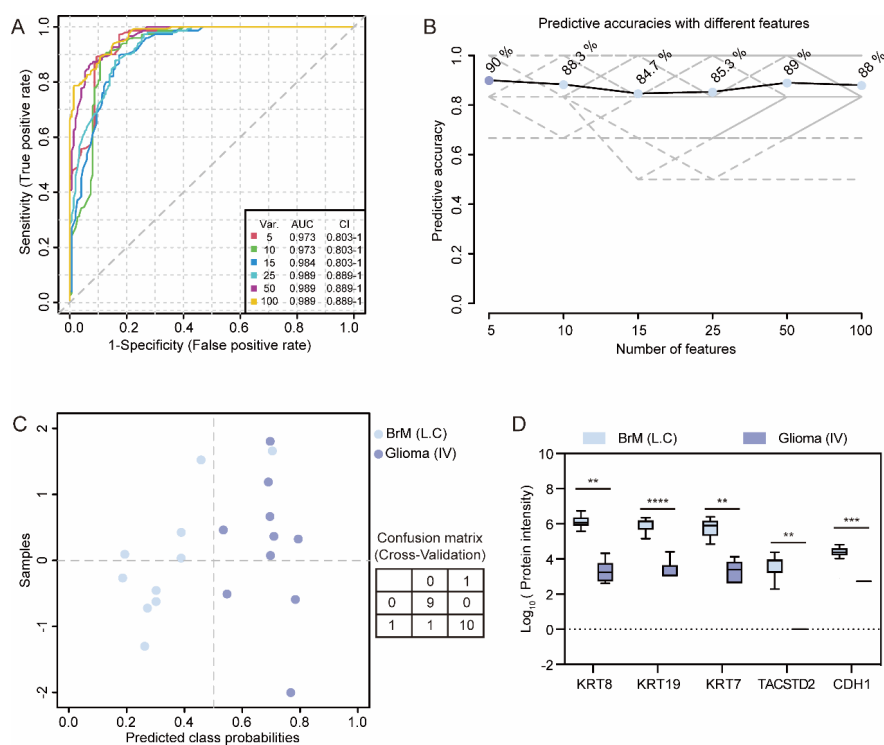


FIGURE 6 Determination of biomarker combinations for distinguishing primary and secondary tumors. **A** Receiver operating characteristic (ROC) curves for all biomarker combination models for discriminating BrMs (L.C) from gliomas (IV) based on Monte-Carlo cross-validation (MCCV). Partial least squares discriminant analysis (PLS-DA) was used as the classification method, and PLS-DA built-in was selected as the feature-ranking method with two set latent variables. **B** Predictive accuracies with different features (top 5, 10, 15, 25, 50, and 100 proteins) based on the ROC curves (A). **C** Predicted class probabilities (average of the

cross-validation) for each sample using a 5-biomarker combination model. Due to balanced subsampling, the classification boundary is at the center ($x = 0.5$, dotted line). **D** Protein intensities of five markers (KRT8, KRT19, KRT7, TACSTD2, and CDH1) in both groups. Box plots represent the median and IQR, and the whiskers represent the 1–99 percentile (two-tailed Student’s t-test, * $P < 0.05$, ** $P < 0.01$, *** $P < 0.001$, and **** $P < 0.0001$).

4 DISCUSSION

BrMs and gliomas, representing two distinct types of brain malignancies, are mostly fatal tumors and are accompanied by poor prognosis. In addition, clinical and biological variability is thought to exist within each type and each grade of tumor, suggesting that the identification of molecular factors that contribute to this variation is invaluable for the development of targeted therapies.

To reveal the common denominators of brain colonization by widely different types of BrMs, we summed up three clusters with distinct protein patterns by unsupervised clustering. Proteins related to tumor proliferation and immune response were recognized as commonalities for metastatic cells to colonize the brain. Among them, the L1 cell adhesion molecule (L1CAM) interaction process was enriched by Reactome pathways in both cluster 1 and 2, but the enrichment was more significant in cluster 1 (Figure 3B). L1CAM is a member of the immunoglobulin-like cell-adhesion molecule family, which has been reported to promote motility and invasion in many tumor vasculatures, including BrMs [31, 32]. Additionally, collagen proteins (e.g., COL18A1, COL4A1, and COL6A1) in extracellular matrix (ECM), which have been recognized as diagnostic tumor markers, were also in cluster 1 (Figure S2C and D). The accumulation of collagens can establish tumorigenesis and metastasis [33–35]. Moreover, the VEGFA-VEGFR2 signaling pathway was present in all clusters, especially in cluster 2. Vascular endothelial growth factor (VEGF)-related pathways stimulate angiogenesis for tumor colonization, and they have been observed in many tumors, including BrMs [15, 36, 37]. In cluster 3, a series of eukaryotic initiation factors (eIFs) that cooperate with ribosomes for mRNA translation was identified (Figure 3D). Because mis-regulated mRNA expression is a common feature of tumor growth, eIFs are aberrantly expressed in many human cancers and serve as potential drug targets in cancer therapy [38]. In addition, subunits of chaperonin-containing tailless complex polypeptide 1 (CCT or TRiC) in cluster 3 play a key role in mediating protein folding and cytoskeleton assembly, which may influence tumor division, migration, and invasion [39].

Among gliomas, when comparing IV-Mut subgroups to II/III-Mut subgroups, nesprin-1 (SYNE1, 4.18 times lower in IV-Mut vs. II/III-Mut) has previously been identified as a frequently high-mutated gene in GBM patients and associated with poor survival [40–42]. Similarly, low glycine decarboxylase (GLDC, 13.48 times lower in IV-Mut vs. II/III-Mut) expression in IV-Mut increases the toxic production of aminoacetone and methylglyoxal, resulting in short survival [43, 44]. Another downregulated protein in IV-Mut, namely, serum deprivation response protein (SDPR or CAVIN2, 10.22 times lower in IV-Mut vs. II/III-Mut), has also been reported to be correlated with poor survival in patients [45]. Conversely, CD14 (4.25 times higher in IV-Mut vs. II/III-Mut) is widely expressed in gliomas, as detected by immunohistochemistry, and the number of CD14⁺ cells increases as gliomas progress [46, 47]. TFc fragment of IgG binding protein (FCGBP, 68.19 times higher in IV-Mut vs. II/III-Mut) has been demonstrated to participate in tumor immunity and is expressed in different grades of gliomas, especially in high-grade gliomas [48]. Similarly, the expression of mitogen-activated protein kinase (MEK1 or MAP2K1, 2.18 times higher in IV-Mut vs. II/III-Mut) is positively correlated with the grade of glioma as MEK1 activates downstream RAS/MAPK signaling pathway for tumor proliferation and invasion, thereby supporting the current use of MEK inhibitors for glioma therapy [49, 50]. In addition, there were several significantly changed proteins (e.g., PPIF, PRSS1, PTRHD1, and PDLIM2; Figure S3D) that have not been reported in glioma research but are regarded as drug targets for other diseases. For instance, PDZ and LIM domain protein 2 (PDLIM2) regulates transcriptional factors in multiple cancers, such as B.C, L.C, and kidney cancer [51] and it has been explored as a therapeutic target for cancer treatment. Thus, PDLIM2 may be used as a novel diagnostic marker to differentiate high-grade gliomas from low-grade formations, and it may even a drug target for gliomas. In addition, comparison of the DEPs in the low-grade versus high-grade group (IV-Mut vs. II/III-Mut) and in the *IDH1* mutant

versus wild-type group (IV-Mut vs. IV-WT) resulted in a low overlap between the two cohorts (cure S3F). Therefore, these results suggested that the proteomics results are reliable and applicable for discriminating different types of gliomas.

The present study utilized BrMs and gliomas to comprehensively analyze primary and secondary brain tumors. Proteomic analysis revealed distinct pathway-level differences between the two types of brain malignancies, in which BrMs focused on tumor development and gliomas progressed to invasiveness. Notably, microenvironment analysis has shown that BrM samples have a more pronounced accumulation of lymphocytes and neutrophils compared to gliomas, whereas gliomas are dominated by microglia [17]. Furthermore, the proteomic differences of BrM (L.C) and glioma (IV) were utilized for precise disease classification. By attempting machine learning, five proteins (KRT8, KRT19, KRT7, TACSTD2, and CDH1) were furtherly selected to classify these two tumors with an accuracy of 90%. In particular, three of these proteins, namely, KRT8, KRT19, and KRT7, belong to the keratin family. Keratins, including KRT7, KRT8, and KRT19, are extensively used as diagnostic tumor markers as malignancies largely maintain the specific keratin patterns associated with their respective cells of origin [52]. Tumor-associated calcium signal transducer 2 (TACSTD2 or TROP2) is a transmembrane glycoprotein that is highly expressed in various cancer types [53]. In the present study, TACSTD2 was overexpressed in BrM (L.C) compared to glioma (IV), suggesting that it may be a candidate marker to differentiate the two cancer types. Another transmembrane glycoprotein, cadherin 1 (CDH1 or E-cadherin), has also been demonstrated to be upregulated in secondary metastases [54]. In summary, these five biomarkers have been validated to be dysregulated in other cancers, and the present study revealed their potential capacity for distinguishing glioma (IV) and BrM (L.C).

Here, we built a comprehensive and comparative proteomic analysis for both BrMs and gliomas for the first time, which uncover the different proteome patterns of these two typical malignant tumors in the brain, indicating potential application in cancer-specific therapy. Further efforts can focus on biomarker validation with more clinical samples.

5 ASSOCIATED DATA

The mass spectrometry proteomics data have been deposited to the ProteomeXchange Consortium (<http://proteomecentral.proteomexchange.org>) via the iProX partner repository [55] with the dataset identifier PXD033881.

ACKNOWLEDGMENTS

We express our appreciation to all the participants for donating tissue samples and providing their clinical characteristics for this study. We are grateful to all the doctors involved in the diagnosis and treatment of these patients. We thank the proteomics and mass spectrometry platform of Institutes of Biomedical Sciences, Fudan University.

CONFLICTS OF INTEREST

The authors declare that the research was conducted in the absence of any commercial or financial relationships that could be construed as a potential conflict of interest.

Funding information

This work was supported by grants from the National Natural Science Foundation of China (grant numbers 81827901, 21874026, and 82001261); the National Key R&D Program of China (grant numbers 2021YFA1301601 and 2017YFA0505100); and the Shanghai Sailing Program (grant number 20YF1403800).

Authors' contributions

Conceptualization, X.L. and L.B.; methodology, X.L. and S.Y.; formal analysis, L.Z. and S.Y.; investigation, C.Z. and S.Y.; resources, L.B., Y.Z. and C.Z.; data curation, L.Z., C.Z. and S.Y.; writing—original draft preparation, S.Y.; writing—review and editing, X.L., L.B., C.Z., L.Z., Y.X. and Y.Z.; visualization, S.Y.;

supervision, X.L. and L.B.; funding acquisition, X.L. and L.B.; software, Y.X. and S.Y. All authors read and approved the final manuscript.

Clinical relevance

Malignant brain tumors, whether primary or secondary, are among the deadliest cancers with poor prognosis and short patient survival. Despite advances in understanding the driver gene mutation and heterogeneity within tumor cells, there is limited information about proteomic changes. The aim of our study was to construct a systemic proteome of those two typical malignant tumors in human brain: primary (gliomas) and secondary (brain metastases) tumors, and dig out their heterogeneities for disease type-specific diagnosis and therapy. In the current work, conserved protein patterns were found in brain metastases. Among gliomas, proteomic heterogeneities were confirmed in different grades of gliomas, which can serve as novel diagnostic biomarkers for glioma subgrouping. In addition, distinct pathway-level differences among two types of brain malignancies were firstly summarized, and five newly discovered proteins were recognized as candidate biomarker to discriminate primary and secondary tumors.

List of abbreviations

AUC: Area under the curve; B.C: Breast cancer; BBB: Blood-brain barrier; BrM: Brain metastasis; C.C: Colorectal cancer; CCT: Chaperonin-containing tailless complex polypeptide 1; CDH1: Cadherin 1; CNS: Central nervous system; CT: Computed tomography; CV: Coefficient of variation; DEP: Differentially expressed protein; ECM: Extracellular matrix; eIF: Eukaryotic initiation factor; FCGBP: Tfc fragment of IgG binding protein; GBM: Glioblastoma; GLDC: Glycine decarboxylase; GSEA: Gene set enrichment analysis; GSM: Gliosarcoma; H: HeLa; IDH: Isocitrate dehydrogenase; IQR: Interquartile range; L.C: Lung cancer; L1CAM: L1 cell adhesion molecule; LC-MS/MS: Liquid chromatography tandem mass spectrometry; LFQ : Label free quantification; MCCV: Monte-Carlo cross-validation; MEK1: Mitogen-activated protein kinase; MRI: Magnetic resonance imaging; MS: Mass spectrometry; Mut: Mutation; O.C: Ovarian cancer; PCA: Principal component analysis; PDLIM2: PDZ and LIM domain protein 2; PLS-DA: Partial least squares discriminant analysis; PSM: Propensity score matching; QC: Quality control; ROC: Receiver operating characteristic; RP: Ribosomal protein; SDPR: Serum deprivation response protein; SYNE1: Nesprin-1; TACSTD2: Tumor-associated calcium signal transducer 2; TIC: Total ion current; VEGF: Vascular endothelial growth factor; WT: Wild type.

References

1. Lah TT, Novak M, Breznik B. Brain malignancies: Glioblastoma and brain metastases. *Semin Cancer Biol.* 2020;60:262-73.
2. Louis DN, Ohgaki H, Wiestler OD, Cavenee WK, Burger PC, Jouvet A, Scheithauer BW, Kleihues P. The 2007 WHO classification of tumours of the central nervous system. *Acta Neuropathol.* 2007;114(2):97-109.
3. Ostrom QT, Gittleman H, Stetson L, Virk SM, Barnholtz-Sloan JS. Epidemiology of gliomas. *Cancer Treat Res.* 2015;163:1-14.
4. Louis DN, Perry A, Reifenberger G, von Deimling A, Figarella-Branger D, Cavenee WK, Ohgaki H, Wiestler OD, Kleihues P, Ellison DW. The 2016 World Health Organization Classification of Tumors of the Central Nervous System: a summary. *Acta Neuropathol.* 2016;131(6):803-20.
5. Tom MC, Cahill DP, Buckner JC, Dietrich J, Parsons MW, Yu JS. Management for Different Glioma Subtypes: Are All Low-Grade Gliomas Created Equal? *Am Soc Clin Oncol Educ Book.* 2019;39:133-45.
6. Aldape K, Brindle KM, Chesler L, Chopra R, Gajjar A, Gilbert MR, Gottardo N, Gutmann DH, Hargrave D, Holland EC, Jones DTW, Joyce JA, Kearns P, Kieran MW, Mellinghoff IK, Merchant M, Pfister SM, Pollard SM, Ramaswamy V, Rich JN, Robinson GW, Rowitch DH, Sampson JH, Taylor MD, Workman P, Gilbertson RJ. Challenges to curing primary brain tumours. *Nat Rev Clin Oncol.* 2019;16(8):509-20.
7. Cagney DN, Martin AM, Catalano PJ, Redig AJ, Lin NU, Lee EQ, Wen PY, Dunn IF, Bi WL, Weiss

- SE, Haas-Kogan DA, Alexander BM, Aizer AA. Incidence and prognosis of patients with brain metastases at diagnosis of systemic malignancy: a population-based study. *Neuro Oncol.* 2017;19(11):1511-21.
8. Lin X, DeAngelis LM. Treatment of Brain Metastases. *J Clin Oncol.* 2015;33(30):3475-84.
9. Fink JR, Muzi M, Peck M, Krohn KA. Multimodality Brain Tumor Imaging: MR Imaging, PET, and PET/MR Imaging. *J Nucl Med.* 2015;56(10):1554-61.
10. Suh JH, Kotecha R, Chao ST, Ahluwalia MS, Sahgal A, Chang EL. Current approaches to the management of brain metastases. *Nat Rev Clin Oncol.* 2020;17(5):279-99.
11. Nejo T, Mende A, Okada H. The current state of immunotherapy for primary and secondary brain tumors: similarities and differences. *Jpn J Clin Oncol.* 2020;50(11):1231-45.
12. Brastianos PK, Carter SL, Santagata S, Cahill DP, Taylor-Weiner A, Jones RT, Van Allen EM, Lawrence MS, Horowitz PM, Cibulskis K, Ligon KL, Taberero J, Seoane J, Martinez-Saez E, Curry WT, Dunn IF, Paek SH, Park SH, McKenna A, Chevalier A, Rosenberg M, Barker FG, 2nd, Gill CM, Van Hummelen P, Thorner AR, Johnson BE, Hoang MP, Choueiri TK, Signoretti S, Sougnez C, Rabin MS, Lin NU, Winer EP, Stemmer-Rachamimov A, Meyerson M, Garraway L, Gabriel S, Lander ES, Beroukhi R, Batchelor TT, Baselga J, Louis DN, Getz G, Hahn WC. Genomic Characterization of Brain Metastases Reveals Branched Evolution and Potential Therapeutic Targets. *Cancer Discov.* 2015;5(11):1164-77.
13. Fukumura K, Malgulwar PB, Fischer GM, Hu X, Mao X, Song X, Hernandez SD, Zhang XH, Zhang J, Parra ER, Yu D, Debeb BG, Davies MA, Huse JT. Multi-omic molecular profiling reveals potentially targetable abnormalities shared across multiple histologies of brain metastasis. *Acta Neuropathol.* 2021;141(2):303-21.
14. Johnson KC, Anderson KJ, Courtois ET, Gujar AD, Barthel FP, Varn FS, Luo D, Seignon M, Yi E, Kim H, Estecio MRH, Zhao D, Tang M, Navin NE, Maurya R, Ngan CY, Verburg N, de Witt Hamer PC, Bulsara K, Samuels ML, Das S, Robson P, Verhaak RGW. Single-cell multimodal glioma analyses identify epigenetic regulators of cellular plasticity and environmental stress response. *Nat Genet.* 2021;53(10):1456-68.
15. Schaffenrath J, Wyss T, He L, Rushing EJ, Delorenzi M, Vasella F, Regli L, Neidert MC, Keller A. Blood-brain barrier alterations in human brain tumors revealed by genome-wide transcriptomic profiling. *Neuro Oncol.* 2021;23(12):2095-106.
16. Gonzalez H, Mei W, Robles I, Hagerling C, Allen BM, Hauge Okholm TL, Nanjaraj A, Verbeek T, Kalavacherla S, van Gogh M, Georgiou S, Daras M, Phillips JJ, Spitzer MH, Roose JP, Werb Z. Cellular architecture of human brain metastases. *Cell.* 2022;185(4):729-45 e20.
17. Klemm F, Maas RR, Bowman RL, Kornete M, Soukup K, Nassiri S, Brouland JP, Iacobuzio-Donahue CA, Brennan C, Tabar V, Gutin PH, Daniel RT, Hegi ME, Joyce JA. Interrogation of the Microenvironmental Landscape in Brain Tumors Reveals Disease-Specific Alterations of Immune Cells. *Cell.* 2020;181(7):1643-60 e17.
18. Wang D, Eraslan B, Wieland T, Hallstrom B, Hopf T, Zolg DP, Zecha J, Asplund A, Li LH, Meng C, Frejno M, Schmidt T, Schnatbaum K, Wilhelm M, Ponten F, Uhlen M, Gagneur J, Hahne H, Kuster B. A deep proteome and transcriptome abundance atlas of 29 healthy human tissues. *Mol Syst Biol.* 2019;15(2):e8503.
19. Petralia F, Tignor N, Reva B, Koptyra M, Chowdhury S, Rykunov D, Krek A, Ma W, Zhu Y, Ji J, Calinawan A, Whiteaker JR, Colaprico A, Stathias V, Omelchenko T, Song X, Raman P, Guo Y, Brown MA, Ivey RG, Szpyt J, Guha Thakurta S, Gritsenko MA, Weitz KK, Lopez G, Kalayci S, Gumus ZH, Yoo S, da Veiga Leprevost F, Chang HY, Krug K, Katsnelson L, Wang Y, Kennedy JJ, Voytovich UJ, Zhao L, Gaonkar KS, Ennis BM, Zhang B, Baubet V, Tauhid L, Lilly JV, Mason JL, Farrow B, Young N, Leary S, Moon J, Petyuk VA, Nazarian J, Adappa ND, Palmer JN, Lober RM, Rivero-Hinojosa S, Wang LB, Wang JM, Broberg M, Chu RK, Moore RJ, Monroe ME, Zhao R, Smith RD, Zhu J, Robles AI, Mesri M, Boja E, Hiltke T, Rodriguez H, Zhang B, Schadt EE, Mani DR, Ding L, Iavarone A, Wiznerowicz M, Schurer

- S, Chen XS, Heath AP, Rokita JL, Nesvizhskii AI, Fenyo D, Rodland KD, Liu T, Gygi SP, Paulovich AG, Resnick AC, Storm PB, Rood BR, Wang P, Children's Brain Tumor N, Clinical Proteomic Tumor Analysis C. Integrated Proteogenomic Characterization across Major Histological Types of Pediatric Brain Cancer. *Cell*. 2020;183(7):1962-85 e31.
20. Kulak NA, Pichler G, Paron I, Nagaraj N, Mann M. Minimal, encapsulated proteomic-sample processing applied to copy-number estimation in eukaryotic cells. *Nat Methods*. 2014;11(3):319-24.
21. Chong J, Soufan O, Li C, Caraus I, Li S, Bourque G, Wishart DS, Xia J. MetaboAnalyst 4.0: towards more transparent and integrative metabolomics analysis. *Nucleic Acids Res*. 2018;46(W1):W486-W94.
22. Zhou Y, Zhou B, Pache L, Chang M, Khodabakhshi AH, Tanaseichuk O, Benner C, Chanda SK. Metascape provides a biologist-oriented resource for the analysis of systems-level datasets. *Nat Commun*. 2019;10(1):1523.
23. Shannon P, Markiel A, Ozier O, Baliga NS, Wang JT, Ramage D, Amin N, Schwikowski B, Ideker T. Cytoscape: a software environment for integrated models of biomolecular interaction networks. *Genome Res*. 2003;13(11):2498-504.
24. Welch DR, Hurst DR. Defining the Hallmarks of Metastasis. *Cancer Research*. 2019;79(12):3011-27.
25. Kalinina J, Peng J, Ritchie JC, Van Meir EG. Proteomics of gliomas: initial biomarker discovery and evolution of technology. *Neuro Oncol*. 2011;13(9):926-42.
26. Pienkowski T, Kowalczyk T, Kretowski A, Ciborowski M. A review of gliomas-related proteins. Characteristics of potential biomarkers. *Am J Cancer Res*. 2021;11(7):3425-44.
27. Aldape K, Zadeh G, Mansouri S, Reifenberger G, von Deimling A. Glioblastoma: pathology, molecular mechanisms and markers. *Acta Neuropathol*. 2015;129(6):829-48.
28. Chen R, Smith-Cohn M, Cohen AL, Colman H. Glioma Subclassifications and Their Clinical Significance. *Neurotherapeutics*. 2017;14(2):284-97.
29. Liu H-j, Hu H-m, Li G-z, Zhang Y, Wu F, Liu X, Wang K-y, Zhang C-b, Jiang T. Ferroptosis-Related Gene Signature Predicts Glioma Cell Death and Glioma Patient Progression. *Frontiers in Cell and Developmental Biology*. 2020;8.
30. Zhuo S, Chen Z, Yang Y, Zhang J, Tang J, Yang K. Clinical and Biological Significances of a Ferroptosis-Related Gene Signature in Glioma. *Frontiers in Oncology*. 2020;10.
31. Altevogt P, Doberstein K, Fogel M. L1CAM in human cancer. *Int J Cancer*. 2016;138(7):1565-76.
32. Angiolini F, Cavallaro U. The Pleiotropic Role of L1CAM in Tumor Vasculature. *Int J Mol Sci*. 2017;18(2).
33. Ricard-Blum S. The collagen family. *Cold Spring Harb Perspect Biol*. 2011;3(1):a004978.
34. Eble JA, Niland S. The extracellular matrix in tumor progression and metastasis. *Clin Exp Metastasis*. 2019;36(3):171-98.
35. Teglas V, Csury DT, Dezso K, Bugyik E, Szabo V, Szallasi Z, Paku S, Reiniger L. Origin and Distribution of Connective Tissue and Pericytes Impacting Vascularization in Brain Metastases With Different Growth Patterns. *J Neuropathol Exp Neurol*. 2019;78(4):326-39.
36. Claesson-Welsh L, Welsh M. VEGFA and tumour angiogenesis. *J Intern Med*. 2013;273(2):114-27.
37. Shen M, Jiang YZ, Wei Y, Ell B, Sheng X, Esposito M, Kang J, Hang X, Zheng H, Rowicki M, Zhang L, Shih WJ, Celia-Terrassa T, Liu Y, Cristea I, Shao ZM, Kang Y. Tinagl1 Suppresses Triple-Negative Breast Cancer Progression and Metastasis by Simultaneously Inhibiting Integrin/FAK and EGFR Signaling. *Cancer Cell*. 2019;35(1):64-80 e7.

38. Hao P, Yu J, Ward R, Liu Y, Hao Q, An S, Xu T. Eukaryotic translation initiation factors as promising targets in cancer therapy. *Cell Commun Signal*. 2020;18(1):175.
39. Vallin J, Grantham J. The role of the molecular chaperone CCT in protein folding and mediation of cytoskeleton-associated processes: implications for cancer cell biology. *Cell Stress Chaperones*. 2019;24(1):17-27.
40. Masica DL, Karchin R. Correlation of somatic mutation and expression identifies genes important in human glioblastoma progression and survival. *Cancer Res*. 2011;71(13):4550-61.
41. Seroo NV, Delfino KR, Southey BR, Beever JE, Rodriguez-Zas SL. Cell cycle and aging, morphogenesis, and response to stimuli genes are individualized biomarkers of glioblastoma progression and survival. *BMC Med Genomics*. 2011;4:49.
42. Xie ZC, Wu HY, Dang YW, Chen G. Role of alternative splicing signatures in the prognosis of glioblastoma. *Cancer Med*. 2019;8(18):7623-36.
43. Kim D, Fiske BP, Birsoy K, Freinkman E, Kami K, Possemato RL, Chudnovsky Y, Pacold ME, Chen WW, Cantor JR, Shelton LM, Gui DY, Kwon M, Ramkissoon SH, Ligon KL, Kang SW, Snuderl M, Vander Heiden MG, Sabatini DM. SHMT2 drives glioma cell survival in ischaemia but imposes a dependence on glycine clearance. *Nature*. 2015;520(7547):363-7.
44. Tiwari V, Daoud EV, Hatanpaa KJ, Gao A, Zhang S, An Z, Ganji SK, Raisanen JM, Lewis CM, Askari P, Baxter J, Levy M, Dimitrov I, Thomas BP, Pinho MC, Madden CJ, Pan E, Patel TR, DeBerardinis RJ, Sherry AD, Mickey BE, Malloy CR, Maher EA, Choi C. Glycine by MR spectroscopy is an imaging biomarker of glioma aggressiveness. *Neuro Oncol*. 2020;22(7):1018-29.
45. Wang Y, Song Z, Leng P, Liu Y. A systematic analysis reveals gene expression alteration of serum deprivation response (SDPR) gene is significantly associated with the survival of patients with cancer. *Oncol Rep*. 2019;42(3):1161-72.
46. Deininger MH, Meyermann R, Schluesener HJ. Expression and release of CD14 in astrocytic brain tumors. *Acta Neuropathol*. 2003;106(3):271-7.
47. Takenaka MC, Gabriely G, Rothhammer V, Mascanfroni ID, Wheeler MA, Chao CC, Gutierrez-Vazquez C, Kenison J, Tjon EC, Barroso A, Vandeventer T, de Lima KA, Rothweiler S, Mayo L, Ghannam S, Zandee S, Healy L, Sherr D, Farez MF, Prat A, Antel J, Reardon DA, Zhang H, Robson SC, Getz G, Weiner HL, Quintana FJ. Control of tumor-associated macrophages and T cells in glioblastoma via AHR and CD39. *Nat Neurosci*. 2019;22(5):729-40.
48. Yan T, Tian D, Chen J, Tan Y, Cheng Y, Ye L, Deng G, Liu B, Yuan F, Zhang S, Cai L, Chen Q. FCGBP Is a Prognostic Biomarker and Associated With Immune Infiltration in Glioma. *Front Oncol*. 2021;11:769033.
49. MacDonald TJ, Brown KM, LaFleur B, Peterson K, Lawlor C, Chen Y, Packer RJ, Cogen P, Stephan DA. Expression profiling of medulloblastoma: PDGFRA and the RAS/MAPK pathway as therapeutic targets for metastatic disease. *Nat Genet*. 2001;29(2):143-52.
50. Ryall S, Tabori U, Hawkins C. Pediatric low-grade glioma in the era of molecular diagnostics. *Acta Neuropathol Commun*. 2020;8(1):30.
51. Guo ZS, Qu Z. PDLIM2: Signaling pathways and functions in cancer suppression and host immunity. *Biochim Biophys Acta Rev Cancer*. 2021;1876(2):188630.
52. Karantza V. Keratins in health and cancer: more than mere epithelial cell markers. *Oncogene*. 2011;30(2):127-38.
53. Lenart S, Lenart P, Smarda J, Remsik J, Soucek K, Benes P. Trop2: Jack of All Trades, Master of None. *Cancers (Basel)*. 2020;12(11).

54. Wong SHM, Fang CM, Chuah LH, Leong CO, Ngai SC. E-cadherin: Its dysregulation in carcinogenesis and clinical implications. *Crit Rev Oncol Hematol*. 2018;121:11-22.

55. Ma J, Chen T, Wu S, Yang C, Bai M, Shu K, Li K, Zhang G, Jin Z, He F, Hermjakob H, Zhu Y. iProX: an integrated proteome resource. *Nucleic Acids Res*. 2019;47(D1):D1211-D7.